nature photonics

REVIEW ARTICLE

PUBLISHED ONLINE: 30 SEPTEMBER 2009 | DOI: 10.1038/NPHOTON.2009.184

Nanowire photonics

Ruoxue Yan[1,2], Daniel Gargas[1,2] and Peidong Yang[1,2]*

Semiconductor nanowires, by definition, typically have cross-sectional dimensions that can be tuned from 2–200 nm, with lengths spanning from hundreds of nanometres to millimetres. These subwavelength structures represent a new class of semiconductor materials for investigating light generation, propagation, detection, amplification and modulation. After more than a decade of research, nanowires can now be synthesized and assembled with specific compositions, heterojunctions and architectures. This has led to a host of nanowire photonic devices including photodetectors, chemical and gas sensors, waveguides, LEDs, microcavity lasers, solar cells and nonlinear optical converters. A fully integrated photonic platform using nanowire building blocks promises advanced functionalities at dimensions compatible with on-chip technologies.

Photonics involves the control of photons in free space or in matter. Manipulation of photons in semiconductor bulk crystals and thin films has culminated in breakthroughs such as LEDs and lasers. The continuing success of photonic technologies relies on the discovery of new optical materials and the miniaturization of optoelectronic devices that feature better performance, low cost and low power consumption. For the past two decades, worldwide efforts in nanomaterials research has led to a rich collection of nanostructures where size, shape and composition can be readily controlled. Many such nanostructures exhibit fascinating optical properties that could have significant impact in the future for photonic technology.

Quantum dots, the commonest example of semiconductor nanostructures, exhibit tunable optical properties. As the quantum dot size decreases, quantum confinement causes the bandgap to increase and this leads to blue-shifted light emission. These three-dimensionally confined nanostructures have been actively investigated for the development of new light-emitting and biological-imaging technologies[1]. However, since the 1990s, another important class of semiconductor nanostructures has emerged: structures with cross-sections of 2–200 nm and lengths upwards of several micrometres. These were initially called 'nanowhiskers'[2], and later 'nanowires'[3]. These structures are different from quantum dots as they are confined only in two dimensions, thus allowing electrons, holes or photons to propagate freely along the third dimension. The high-aspect-ratio of these new semiconductor nanostructures allows for the bridging of the nanoscopic and macroscopic world. This nano–macro interface is fundamental to the integration of nanoscale building blocks in electrical or optoelectronic device applications. Conventional photonic platforms often consist of features with large aspect-ratios such as interconnects and waveguides, typically with micrometre dimensions. Thus, when semiconductor nanowires emerged they were immediately recognized as one of the essential building blocks for nanophotonics.

Since their introduction in the 1990s, semiconductor nanowires have been extensively studied and much insight has been gained on tuning their electrical and optical properties by controlling their size and dimensions. Furthermore, the one-dimensional (1D) nature of nanowires permits materials synthesis in traditionally inaccessible compositional regions, which has been recently demonstrated in single-crystalline InGaN nanowires with a tunable bandgap from the UV to the near-infrared[4]. Such nanowires with tunable electronic structures hold great promise in photovoltaics, solid-state lighting and solar-to-fuel energy conversion. Today, growth techniques for semiconductor nanowires have advanced to a level where desired composition, heterojunctions and architectures can be readily synthesized. The assortment of 1D nanostructured optoelectronic devices includes photodetectors, chemical and gas sensors, waveguides, nonlinear optical converters, LEDs and microcavity lasers.

Nanowire growth

The creation of semiconductor nanowires through a bottom-up approach is heavily dependent on the controlled synthesis of 1D, single-crystalline, high-optical-quality materials. The 'vapour–liquid–solid' (VLS) growth, which promotes seeding and oriented growth by introducing a catalytic liquid alloy phase that can rapidly adsorb a vapour to supersaturation levels, has achieved the most success in producing various semiconductor nanowires in relatively large quantities. Originally proposed by Wagner and co-workers at Bell Laboratories in the early 1960s (ref. 5) to explain gas-phase silicon whisker growth in the presence of a liquid gold droplet, the VLS growth mechanism has been re-examined and developed over the past two decades by Lieber[6,7], Yang[8], Samuelson[9] and many other research groups. In the early 1990s, III–V nanowhiskers were synthesized and investigated by scientists at Hitachi[2]. Recent advances in both physical[6] (laser ablation and thermal evaporation) and chemical deposition techniques (chemical vapour transport and deposition, and metal-catalysed molecular beam epitaxy) have allowed development of a broad range of inorganic nanowire compositions (for example, Si, Ge, ZnO, CdS, GaN, GaAs and InP), including group IV[10,11], II–VI[12,13] and III–V[14,15] compound and alloy crystal structures[4,16,17]. It is also worth mentioning that the Buhro group was able to grow III–V nanowires in a solution environment using a similar solution–liquid–solid process[18].

Understanding of the VLS mechanism has led to nanowire growth with precise control over length, diameter, growth direction[19], morphology and composition. Nanowire diameter, typically from several nanometres to hundreds of nanometres, is determined by the size of the metal alloy droplets. Consequently, nanowire arrays with uniform size can be readily obtained by using monodispersed metal nanoparticles[20]. The length of these nanowires can be easily controlled from micrometres to millimetres. Precise orientation control during nanowire growth can be achieved by applying conventional epitaxial crystal growth techniques to this VLS process, known as vapour–liquid–solid epitaxy. This process is particularly powerful in the controlled synthesis of high-quality nanowire

[1]Department of Chemistry, University of California, Berkeley, California 94720, USA. [2]Materials Sciences Division, Lawrence Berkeley National Laboratory, Berkeley, California 94720, USA. *e-mail: p_yang@berkeley.edu

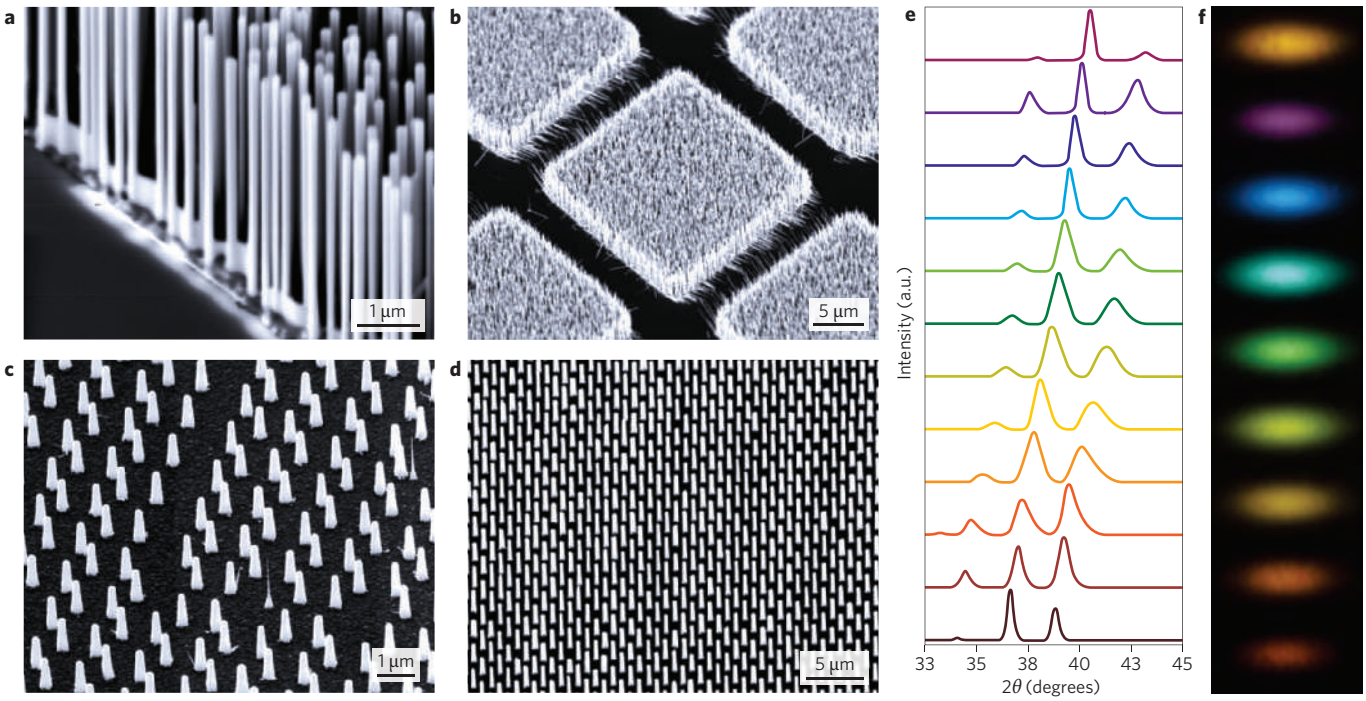

Figure 1 | Semiconductor nanowire growth. a–d, Scanning-electron microscope images of ZnO (**a**), GaN (**b**), InP (**c**) and InP/InAs/InP core–multishell (**d**) nanowire arrays. **e**, X-ray diffraction for InGaN nanowires with different In concentrations, increasing downwards. **f**, CCD camera image of the visible photoluminescence emission of $In_xGa_{1-x}N$ nanowire (x = 0–0.6). Images reproduced with permission from: **b**, ref. 19, © 2007 NPG; **c**, ref. 27, © 2004 ACS; **d**, ref. 36, © 2006 AIP; **e** and **f**, ref. 4, © 2004 NPG.

arrays and single-wire devices[21]. For example, highly oriented ZnO and GaN nanowire arrays can be epitaxially grown on an appropriate substrate such as sapphire or $LiAlO_2$ (Fig. 1a,b). A similar level of growth control has been achieved for III–V systems. Early work at Hitachi demonstrated good positional control of InAs and GaAs nanowires[23,24] through metal thin-film patterning. Within the past 10 years, great progress has been made in understanding the fundamental growth mechanism of III–V nanowires[25,26], as well as in the precise positional control of nanowire growth using advanced lithography processes. Recent work, notably from groups at Lund University and Philips Research Laboratories, has shown beautifully the growth of highly ordered arrays of III–V nanowires with different compositions[27] (Fig. 1c). Importantly, owing to the nature of free-standing nanowire growth, these nanowires and their heterojunctions are usually dislocation-free and can readily accommodate large lattice mismatches, unlike thin-film growth[28]. Therefore, semiconductor nanowire growth also allows direct integration of optically active semiconductors (for example, III–V compounds) onto silicon substrates[29–32]. This capability represents a significant advantage over conventional thin-film technology.

Although the VLS process has been very successful in making semiconductor nanowires of various compositions, the use of metal in the growth process inevitably introduces the potential problem of contamination. This has been a key concern when considering nanowire technologies for the large-scale optoelectronics industry. To mitigate this problem, efforts have been devoted towards nanowire growth without using metal particles or thin films[33]. For example, a team at Hokkaido University has used selective-area metal–organic vapour phase epitaxy to grow ordered arrays of III–V nanowires and their heterojunctions[34–36] (Fig. 1d). This process is free of metal catalysts and therefore effectively avoids the metal contamination issue.

Another important task in semiconductor nanowire synthesis is the precise control and full-range tunability over the composition of doped and alloyed nanowires, which are of particular interest because of their potential applications in high-efficiency solid-state lighting and photovoltaics. Recent progress in our group has demonstrated broad tunability in nanowire synthesis for systems that traditionally have been subject to inevitable phase separation in bulk and thin-film forms, owing to the ability of the nanowire morphology to accommodate strain-relaxed growth. Single-crystalline $In_xGa_{1-x}N$ nanowires have been synthesized across the entire compositional range from x = 0 to 1 by low-temperature halide chemical vapour deposition, and were shown to have tunable emission from the near-UV to the near-infrared region[4] (Fig. 1d,e).

Another critical breakthrough in the development of nanowire building blocks is the controlled growth of nanowire heterostructures, including co-axial[37–40] and longitudinal variations[41–44] (Fig. 2a,b). Typically, direct overgrowth on the side wall of the nanowire leads to co-axial heterostructures, whereas sequential nanowire VLS growth produces longitudinal heterostructures. The ability to form diverse heterostructures sets nanowires apart from other nanomaterials (such as quantum dots and carbon nanotubes) and represents a substantial advantage for the development of increasingly powerful and unique nanoscale electronic and optoelectronic devices[45]. Finally, highly controlled architecture modulation can also be realized through the VLS growth mode to form complex branching structures. For example, single-crystalline GaP 'nanotrees' can be grown through a sequential-seeding technique where each level of branching is controlled in terms of branch length, diameter and density[46]. More recently, it was discovered that highly branched PbS nanowires (Fig. 2c) can be readily synthesized through a dislocation-driven growth mechanism using a simple chemical vapour transport setup[47,48].

Optical assembly of nanowires

Although a high level of composition and orientation control in semiconducting nanowires can be achieved by epitaxial growth, assembling these nanowires into functional and highly integrated 2D or 3D heterogeneous material systems with high spatial and

angular precision remains a major challenge, relying heavily on post-synthesis integration of various nanowires. At present, several post-synthesis nanowire assembly techniques have been investigated, including using electric[49] and magnetic fields, laminar flow in microfluidic channels[50,51], Langmuir–Blodgett compression[52,53] and microcontact printing[54]. Although these techniques opened up the possibility to organize and align macroscopic arrays of nanowires, they lack the ability to address and position single nanostructures with arbitrary precision. The 3D manipulation of single nanowires remains an active area of research in nanowire assembly. Direct manipulation of nanowires in a liquid medium is even more challenging.

One possible approach is to manipulate nanowires with optical tweezers — tightly focused laser beams capable of holding and moving microscopic dielectric objects in three dimensions. Since their introduction in 1986 (ref. 55), the optical tweezer has become an important tool for the manipulation of objects ranging in size from tens of nanometres to tens of micrometres[56]. Optical trapping is particularly appealing for nanowire manipulation and integration because it can be carried out directly in a liquid medium with high spatial-positioning accuracy (<1 nm)[57]. Recent work with a focused, infrared single-beam optical trap has shown that it is possible to optically trap, transfer and assemble high-aspect-ratio semiconductor nanowires into arbitrary structures at room temperature, at both physiological pH and ionic strength[58]. A schematic of the assembly procedure is shown in Fig. 3a,b. Further precision-controlled nanowire arrangements (in two and three dimensions) have been demonstrated by holographic optical trapping[59]. Using these methods, complex and robust nanowire structures that function as active photonic devices can be constructed in physiological environments (Fig. 3c), thereby offering new types of chemical, mechanical and optical probes for studying living cells.

Equally important to the precision control of nanowire assemblies is the massive parallel differentiation and manipulation of individual nanowires with arbitrary composition. In this context, optoelectronic tweezers[60] (OETs) have emerged as a powerful tool for addressing individual semiconducting and metallic nanowires with diameters less than 20 nm, through the optically induced dielectrophoresis force[61]. Compared with optical tweezers, OETs operate at an optical power density that is orders of magnitude lower, transport individual nanowires with much greater speed and are capable of addressing multiple nanowires simultaneously. An individual silicon nanowire with a diameter of 100 nm and a length of 5 μm has a maximum trapping speed that approaches 135 μm s^{-1}, with a peak-to-peak trapping voltage of 20 V. This is approximately four times the maximum speed achievable by optical tweezers, and is reached with an optical power density 5–6 orders of magnitude less than optical tweezers. Figure 3d–f shows the schematic of an OET device structure with an individual nanowire trapped at the laser spot and a large array of silver nanowires assembled with traps created by photopatterned virtual electrodes. Adding to the merits of an OET is the ability to separate semiconducting and metallic nanowires, which suggests a broad range of applications for the separation and heterogeneous integration of 1D nanoscale materials.

To realize the integration of nanowires into large-scale optoelectronic devices and systems, assembly techniques that are scalable, massively parallel, low cost and high throughput must be developed. In particular, addressability and precise registration of individual features within a multilayer optoelectronic platform remains a challenge. Unfortunately, none of the existing assembly techniques provide a complete solution to this problem, and this is believed to be one of the potential road blocks that will dictate whether any of the nanowire electronic or optoelectric technologies can eventually become commercially viable.

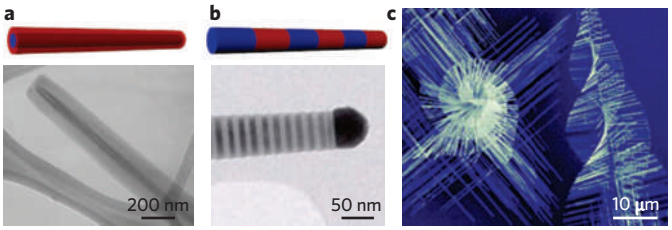

Figure 2 | Semiconductor nanowire heterojunctions. a, Schematic (top) and transmission electron microscope (TEM) image of a GaN/AlGaN core–sheath nanowire. **b**, Schematic (top) and TEM image of an InP superlattice nanowire. **c**, Scanning-electron microscope image of highly branched PbS nanowires. Images reproduced with permission from: **a**, ref. 37, © 2003 ACS; **b**, ref. 41, © 2008 NPG; **c**, ref. 47, © 2008 AAAS.

Nanowire lasers/LEDs

Inorganic semiconductor nanowires represent a class of important nanostructures as optical gain media that could potentially outperform their thin-film counterpart. The unique characteristics of semiconductor nanowires, such as their 1D geometry, dislocation-free single-crystalline nature, high index of refraction and atomically smooth surface, allow for sufficient end-facet reflectivity and photon confinement in a volume of just a few cubic wavelengths of material. So far, optically pumped coherent laser emission has been detected from a number of different nanocavities of binary semiconductors, including ZnO ($\lambda \sim 385$ nm) epitaxial arrays[22], combs[62], tetrapods[63], single nanowires and nanoribbons[64], ZnS (~337 nm)[65] nanoribbons, CdS (~490 nm)[66], GaN (~375 nm)[67] and GaSb (~1,550 nm)[68] nanowires, and GaN ring resonators[69]. Nanowire lasing under optical pumping was first observed in ZnO by the Yang group[22]. Since then, nanowire photonics has branched into many research avenues. Well-faceted nanowires with diameters of 100–500 nm support predominantly axial Fabry–Pérot waveguide modes, separated by $\Delta\lambda = \lambda^2/[2Ln(\lambda)]$, where L is the cavity length and $n(\lambda)$ is the group index of refraction (Fig. 4a). Significant scattering loss prevents smaller wires from lasing. The large refractive index difference between the semiconductor material and its surrounding dielectric environment enables photonic confinement in the nanowire cavities. These structures act as waveguides for specific axially guided modes and provide sufficient resonant feedback for low-gain threshold values and high quality factors. Hence, modal gain in nanowires can be achieved and the nanowires can serve as excellent resonant cavities for light amplification. Typical output of an optically pumped, single ZnO nanowire laser was recently measured to be several tens of microwatts[70]. By placing these nanowires in external cavities such as photonic crystals[71] or fabricating distributed Bragg reflectors with high reflectivity, it is possible to further reduce their lasing threshold. Far-field imaging indicates that photoluminescence and lasing emission are localized at the ends of nanowires, which suggests strong waveguiding behaviour that is consistent with axial Fabry–Pérot modes (Fig. 4c). Theoretical simulation of the nanowire far-field emission predicts that the angular emission intensity of these nanowire lasers is highly dependent on the mode type within (that is, transverse electric, transverse magnetic, or a hybrid of the two[72]). Analysis of the interference pattern[73] from the wire end-facets suggests that the nanowire laser emission might be non-directional. This is in contrast with macroscopic lasers, where directional emission is expected.

Beyond nanowire lasers, confined core–sheath nanowire heterostructures provide a unique geometry for applications in optoelectronics. Quantum confinement has measurable effects if the diameter of the gain medium is reduced in size below the Bohr exciton radius of the semiconductor. Effective carrier/exciton confinement has been demonstrated for a core–sheath GaN/AlGaN heterostructure (Fig. 2a), in which the active GaN material has a diameter as small as

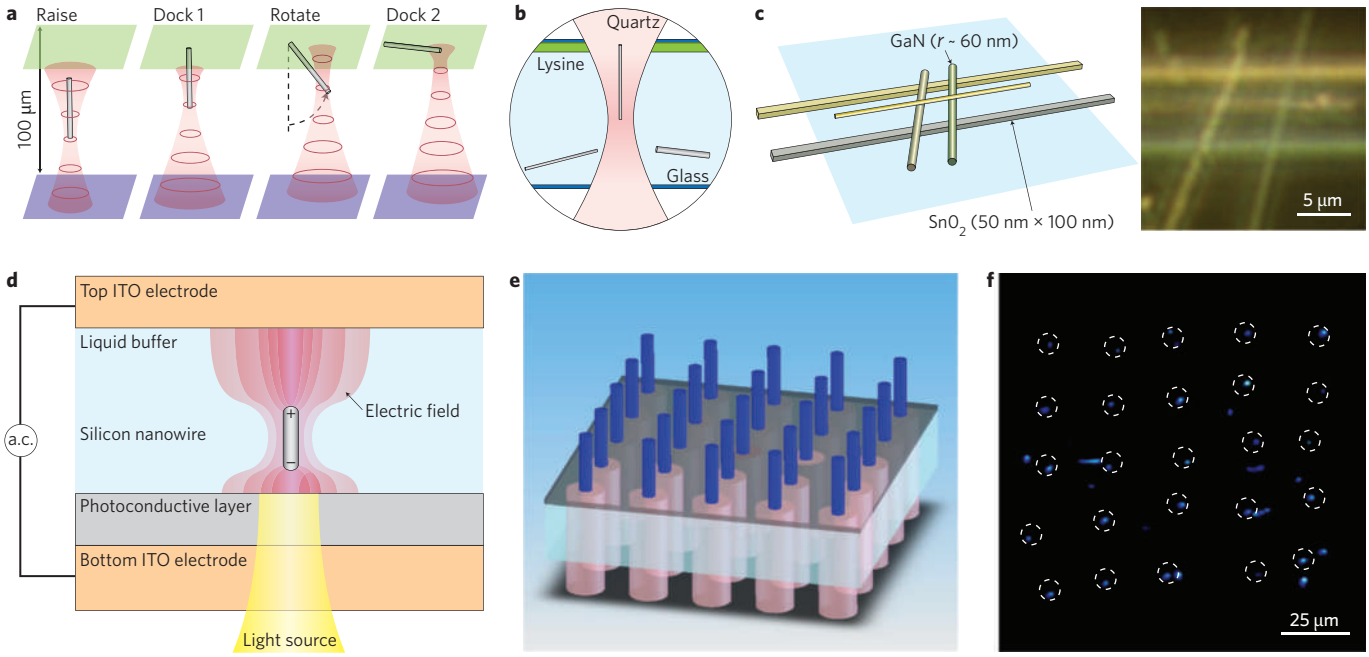

Figure 3 | Nanowire assembly with optical trapping. a, Schematic of optical trapping procedure for nanowire docking at a surface. An individual nanowire is pulled to the centre of the optical trap through optical forces, then is raised to the top surface of the trapping chamber (dock 1) and translated laterally until it is deposited horizontally on the top surface (dock 2). **b**, Schematic of an experimental chamber cross-section. The top surface consists of a fused silica coverslip (blue) coated with lysine or gold (green). **c**, Schematic (left) and optical dark-field image (right) of a three-dimensional nanowire assembly consisting of SnO_2 nanoribbons and GaN nanowires in a fluid chamber. **d**, Optoelectronic tweezer device structure with an individual nanowire trapped at the laser spot. Typical laser intensity used here is about 100 W cm^{-2}. ITO; indium tin oxide. **e**,**f**, 5 × 5 single silver nanowire array formed using traps created with a digital micromirror spatial light modulator. Images reproduced with permission from: **a**–**c**, ref. 58, © 2006 NPG; **d**–**f**, ref. 61, © 2008 NPG.

5 nm and is surrounded by a thick sheath of $Al_{0.75}Ga_{0.25}N$ (which has a larger bandgap and lower refractive index than the GaN core[37]), creating a structure with simultaneous exciton and photon confinement (waveguiding). When optically pumped, the core functions as a gain medium and the sheath serves as a Fabry–Pérot optical cavity. Recently, room-temperature tunable lasing has been demonstrated in multi-quantum-well (MQW) core–shell nanowire heterostructures[39] (Fig. 4b). The co-axial heterostructure consists of a GaN nanowire core, which functions as the primary part of the optical cavity, and epitaxial InGaN/GaN MQW shells, which serve as the composition-tunable gain medium. Optical excitation of individual MQW nanowire structures yielded lasing with InGaN quantum-well composition-dependent emission of 365–494 nm (Fig. 4d). Similarly, near-infrared lasing has also been demonstrated in GaAs/GaAsP coaxial core–shell nanowires[74–76].

Despite all the progress made in optically pumped nanowire lasing, realization of a reliable, electrically injected nanowire nanolaser[66] remains a major challenge, owing to issues such as the difficulty of fabricating reliable nanoscale metal–semiconductor contacts. Other technical difficulties also include the formation of high-gain heterojunctions or MQWs within single nanowires, and effective surface passivation to eliminate undesirable recombination pathways. It is also unclear at this point what would be the best approach to integrate these nanowire gain materials into a low-loss-cavity design. Although difficult to accomplish, electrically injected nanowire nanolasers could eventually offer many benefits such as low threshold current, low power consumption, large-scale integration and fast modulation bandwidth. Furthermore, because their footprints are comparable to electronic transistors, they are attractive for intra-chip optical interconnect applications.

In addition to optically pumped nanowire lasers, electrically driven spontaneous emission has also been realized repeatedly in nanowire-based LEDs, which often require p- and n-type nanowires to be crossed, or electrical contact to be made to the p- and n- parts of a single heterostructured nanowire. Nanowire LEDs were first demonstrated using the vertical GaAs p–n junction arrays by the Hitachi team[24]. So far, nanowire LEDs have been successfully realized in a variety of crossed-nanowire junctions[77–79], forming longitudinal[80] and co-axial heterostructures[38] with electroluminescence emission ranging from the near-infrared to UV. In particular, multicolour LEDs have been fabricated on a single substrate by crossing different n-type nanowires, including GaN (UV), CdS (green) and CdSe (near-infrared). The p-type material is usually a silicon nanowire or lithographically patterned silicon strips[78], which allow easy interfacing with conventional silicon microelectronics.

Nanowire waveguides and nonlinear optical mixing

In the previous sections, we have discussed the synthesis and assembly of semiconductor nanowires, and the promising developments of these chemically synthesized nanowires into nanoscale light sources (lasers and LEDs). However, to perform logic operations such as in computing, communications and sensing (in future integrated photonic circuits), photons generated by these nanowire light sources must be efficiently captured and precisely delivered to other nanowire optical components that assume various functions, such as photodetectors, frequency converters, filters and switches. The development of nanowire subwavelength waveguides is an important step towards on-chip routing of optical signals to carry out these complex tasks. In contrast with lithographically defined waveguides, chemically synthesized binary oxide nanowires have several features that make them viable photonic waveguides, including inherent one-dimensionality, single crystallinity, large refractive indices, low surface-roughness, high flexibility, large material diversity and, in principle, the ability to operate both above and below the diffraction limit.

Among available oxide nanowires, tin dioxide (SnO_2) nanoribbons have proved to be excellent subwavelength waveguides[81]. These are nanoscale mimics of conventional optical fibres; they have a high refraction index (n = 2.1), typical dimensions of 100–400 nm and can efficiently guide their own visible photoluminescence and visible/UV emissions from other nanowires and fluorophores. Losses range from 1–8 dB mm^{-1} for wavelengths of 450–550 nm, depending on the ribbon's cross-sectional area. These values are higher than those of conventional optical fibres, but are sufficient for integrated planar photonic applications such as short-distance on-chip signal routing and distribution. For example, optical linkages between active nanowires (GaN and ZnO) and passive nanowires (SnO_2) can be formed through tangential evanescent coupling (Fig. 5a,b).

Further to the versatility of SnO_2 nanoribbon waveguides is their excellent application as short-pass filters that exhibit different cut-off wavelengths depending on their cross-section. For example, cross-sectional dimensions of the 465 nm, 492 nm, 514 nm, 527 nm and 580-nm nanowire filters are 310 nm × 100 nm (0.031 μm^2), 280 nm × 120 nm (0.034 μm^2), 350 nm × 115 nm (0.040 μm^2), 250 nm × 225 nm (0.056 μm^2) and 375 nm × 140 nm (0.052 μm^2), respectively. Therefore, nanoribbons of different cut-off frequencies can be integrated with a common multimode core waveguide ribbon to produce an optical router based on input colour. Assemblies such as multibranched hubs and grids have already been implemented in nanowire-based electronic logic, suggesting that similar nanowire architectures could be potentially used in integrated optical logic[82] and all-optical switching[83].

Another advantage that semiconductor nanowires have over their silica counterpart[84] is their ability to efficiently guide light through water and other liquid media, owing to their higher refractive index[85]. This becomes especially important if these nanowires must be interfaced with liquid media for on-chip chemical or biological spectroscopic analysis. A critical issue here is the development of a tunable, coherent radiation source that is stable in physiological conditions. One way of achieving this is to use a nanoscale nonlinear optical mixing component that coherently converts an arbitrary input laser into the desired frequency. This has been recently achieved with individual potassium niobate nanowires[86], which exhibit efficient second-harmonic generation and act as frequency converters, allowing local synthesis of a wide range of colours through sum-frequency generation (Fig. 5c,d). This tunable nanometre-scale light source has also been used to implement a new form of subwavelength microscopy, in which an infrared laser (1,064 nm) is used to optically trap and scan a nanowire over a sample. The availability of such tunable nanoscopic light sources in liquid environment signifies a wide range of potential applications, particularly in the area of biological imaging in physiological environments. Lastly, although it has been demonstrated that it is possible to perform efficient second/third-harmonic generation and sum-frequency generation within single nanowires, it is unclear at this stage whether it is possible to have optical parametric generation/amplification within single nanowires.

Nanowire photodetectors and photovoltaics

Nanostructures that efficiently detect optical inputs and process them as electrical outputs are of great interest for improving nanoscale devices in optoelectronics. A linear nanowire photodetector/switch has been realized in ZnO (ref. 87), InP (ref. 88) and CdS (ref. 89) nanowires fabricated into a horizontal transistor configuration where an optical flux changes the wire from an insulating to a conducting state. The response levels of typical InP nanowire photodetectors are of the order of 3,000 A W^{-1}. For higher photosensitivity at the nanoscale, large amplification is often required to detect low levels of light (that is, single photons) with reasonable response times. Recently, avalanche multiplication of the photocurrent has been reported in nanoscale p–n diodes consisting of

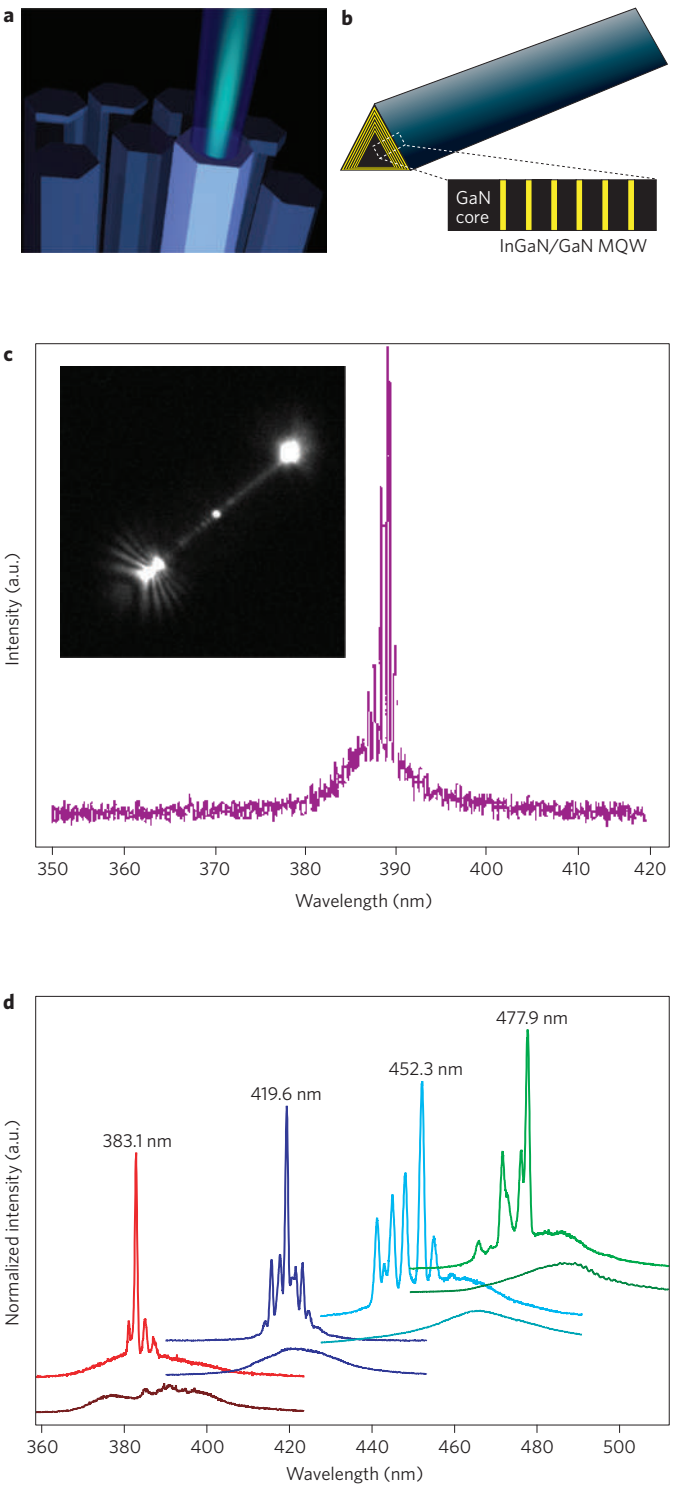

Figure 4 | Nanowire nanolasers. a, Schematic of an optically pumped nanowire laser cavity. **b**, A multi-quantum-well (MQW) nanowire and magnified cross-sectional view of a nanowire facet, highlighting the InGaN/GaN MQW structure. The InGaN layer is indicated in yellow. **c**, Lasing spectrum from an individual ZnO nanowire, and a far-field optical image of a lasing GaN nanowire (inset). **d**, Normalized lasing spectra collected from four representative MQW nanowire structures, with indium composition increasing towards the right. The lower and upper spectra for each sample were obtained by pumping at ~250 kW cm^{-2} and ~700 kW cm^{-2}, respectively. Images in **c** and **d** reproduced with permission from ref. 39, © 2008 NPG.

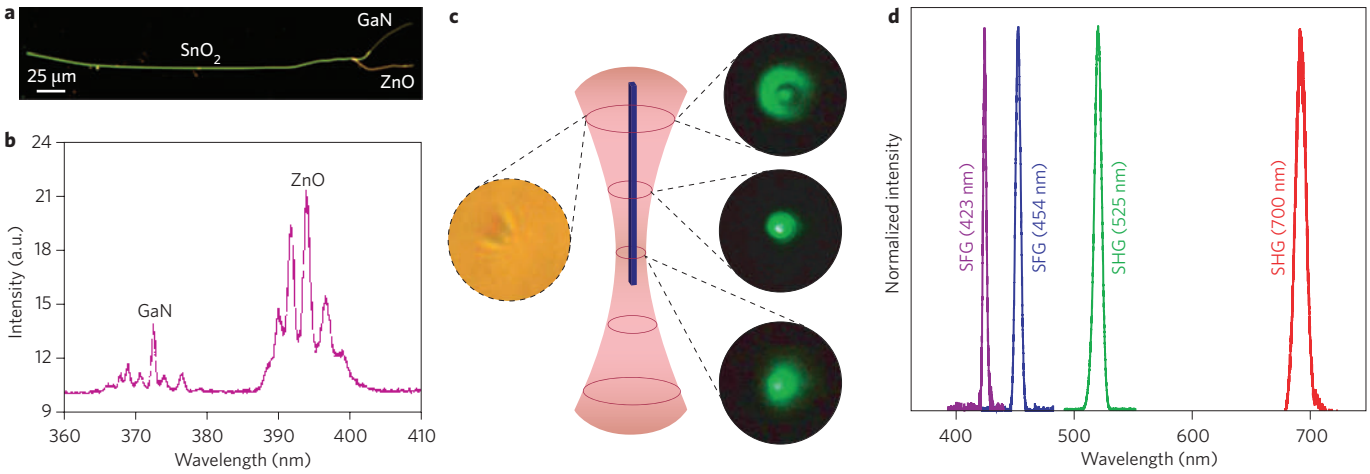

Figure 5 | Nanowire waveguides and nonlinear optical converter. a, Dark-field image illustrating the coupling geometry of two nanowire lasers (GaN and ZnO) to a common SnO_2 nanoribbon waveguide. **b**, Spectra recorded at the left terminus of the SnO_2 nanoribbon after simultaneous nanowire laser injection at the right terminus. Both laser pulses are guided through the SnO_2 waveguide and emerge as two resolvable packets of modes. **c**, Bright field (left) and second-harmonic generation (SHG; right) images of an optically trapped single potassium niobate ($KNbO_3$) nanowire. Waveguiding of the SHG signal (green) leads to diffraction rings at the distal (top) end of the nanowire, which acts as a subwavelength aperture. **d**, Panchromatic wavelengths generated by the nonlinear optical processes (SHG and sum-frequency generation, SFG) within individual $KNbO_3$ nanowires. It shows SFG signals (λ = 423 nm and 454 nm, with 800/900 nm and 800/1,050 nm fundamental beams, respectively) and SHG signals (λ = 525 nm and 700 nm) obtained from a single $KNbO_3$ nanowire by introducing fundamental beams at a variety of different frequencies through a tunable femtosecond pump. Images reproduced with permission from: **a** and **b**, ref. 85, © 2004 AAAS; **c** and **d**, ref. 86, © 2007 NPG.

crossed silicon–cadmium sulphide nanowires[90]. The high-sensitivity nanowire avalanche photodiodes (nanoAPDs) exhibited detection limits of less than 100 photons (for λ <500 nm) and a subwavelength spatial resolution of 250 nm. At present, these nanoAPDs exhibit sensitivities comparable to those reported for conventional planar APD structures. The temporal response of these nanoAPDs was measured to be of the order of several microseconds, which is considerably slower than large-area commercial silicon APDs[91]. It was suggested that using core–shell nanowires could further improve the gain, detection sensitivity and device stability. Furthermore, these nanoAPDs may be fabricated into crossed-nanowire arrays that can be addressed independently without optical signal interference from adjacent nanowires. Such nanoAPDs and arrays offer significant potential in many diverse areas, ranging from nanopositioning, integrated photonics and near-field detection, to real-time observation of single-protein dynamics with integrated nanoAPDs in microfluidics[92].

Another crucial component for the operation of any nanophotonic device is the power supply. Solar cells are promising devices for inexpensive, large-scale solar-energy conversion. When miniaturized, they might also be incorporated directly into nanophotonic systems as integrated power sources to form a self-powered system. The use of semiconductor nanowires for photovoltaic applications is in itself advantageous because: (1) it allows long absorption paths along the length of the wire, yet short distances for carrier collection/transport from the semiconductor interface within the nanowire (that is, light absorption and charge transfer can be orthogonalized); (2) an interpenetrating heterojunction interface is possible at the nanoscale, allowing efficient carrier extraction following light absorption; (3) strong light trapping can be achieved in high-density nanowire arrays; and (4) modification of materials properties and cell efficiencies is possible through size and composition variation of the nanostructures.

The benefit of using nanowire arrays as photoelectrodes was first demonstrated in dye-sensitized solar cells. The anodes of dye-sensitized solar cells[93] are typically constructed using thick films of TiO_2 or ZnO nanoparticles that are deposited as a paste and sintered to achieve electrical continuity. The nanoparticle film provides a large internal surface area for the anchoring of sufficient chromophore (usually a ruthenium-based dye) to yield high light absorption in the 400–800 nm region, where much of the solar flux is incident. During operation, photons intercepted by the dye monolayer create excitons that are split rapidly at the nanoparticle surface — the electrons are injected into the nanoparticle film and the holes leave through the opposite side of the device by means of reduction–oxidation species (traditionally the I^-/I_3^- couple) in a liquid- or solid-state electrolyte. Dye-sensitized solar cells fabricated from dense arrays of oriented, crystalline ZnO nanowires have been designed to improve charge-collection efficiency[94]. The nanowire anode is synthesized using mild aqueous chemistry and has a surface area up to one fifth the size of a typical nanoparticle cell. The direct electrical pathways provided by the single-crystalline nanowires ensure the rapid collection of carriers generated throughout the device, and a full Sun efficiency of 2.5% (ref. 95) has been demonstrated, limited primarily by the surface area of the nanowire array. More recently, coaxial silicon nanowires (p-type/intrinsic/n-type layers, or p-i-n) have yielded an energy conversion efficiency of up to 3.4% under one solar equivalent illumination, and are able to drive functional nanoelectronic sensors and logic gates[96]. These nanowire-based photovoltaic elements might find general use as environmentally friendly, self-integrated power supplies for ultra-low-power nanophotonic and diverse nanosystems. However, the scientific challenge remains as to whether it is possible to design and synthesize nanowires and their heterostructures with improved performance beyond existing silicon photovoltaic technology.

Perspectives

The ability to manipulate pulses of light within submicrometre volumes is vital for highly integrated light-based devices, such as optical computers, to be realized. Chemically synthesized nanowires represent an important class of photonic building blocks that exhibit subwavelength optical functionalities. Although state-of-the-art lithography techniques are capable of fabricating nanostructured features with dimensions discussed in this article, chemically grown nanowires still possess unique advantages of being single-crystalline, relatively defect-free, having atomically smooth surfaces and being

able to accommodate large lattice mismatches. Using a combination of nanolithographic tools, it is highly feasible to assemble photonic circuits from a collection of nanowire elements that assume various functions, such as light generation, routing and detection. Because the range of nanowire material types now include active, passive, nonlinear and semiconducting inorganic crystals, as well as a rich variety of polymers, synthesizing from the bottom up offers new design-by-choice schemes to facilitate the heterogenous assembly of multifunctioning components on the same substrate. Furthermore, because of their small footprint and low power consumption, they can be self-powered and readily embedded in cell phones or wrist-watches.

The past decade has seen tremendous progress in this exciting research field of semiconductor nanowires. However, many fundamental issues and questions still remain. Although it has been demonstrated that nanowires can indeed have many different functionalities such as light emission, lasing, waveguiding and nonlinear optical mixing, it is important that quantitative comparisons be made with conventional thin-film technology in terms of efficiency, fabrication cost and stability. Such benchmarking is important to assess whether this new class of nanostructures is a viable candidate for future generations of photonic technologies. Unfortunately, such benchmarking data is critically lacking at this point. For example, one of the appealing features of nanowires is that they can be single-crystalline, well-faceted with low defects, and have single domains — all of which are critical for high optical quality. On the other hand, nanowires have a significant external surface area, which potentially introduces a high density of surface-trap states that are detrimental for light-emitting processes. Of course, such surface states must be properly passivated, which is especially important in nanowire-based solid-state lighting.

Furthermore, although the rapid development of nanoscience has provided numerous exciting opportunities for electronic and photonic applications, it is also important to point out that certain nanoparticles have proved to be toxic, and nanowires are reminiscent of asbestos and chrysolite. Therefore, a systematic evaluation of the environmental and health implications of the large-scale production of these materials is urgently required[97].

Another powerful approach towards subwavelength photonics is the use of plasmonics that arise at the metal–dielectric interface. For example, a recent theoretical study of a nanowire with a semiconductor-core–metal-shell structure[98] showed that positive modal gain is achievable, demonstrating the feasibility of making a laser with all three dimensions less than one wavelength[99]. This line of research could further lead to the fabrication of single-photon sources and the development of hybrid plasmonic–photonic waveguides with strong mode confinement[100]. Considering such remarkable progress in nanowire photonics, many new discoveries should be expected further down the road.

References

1. Michalet, X. *et al.* Quantum dots for live cells, *in vivo* imaging, and diagnostics. *Science* **307,** 538–544 (2005).
2. Yazawa, M., Koguchi, M. & Hiruma, K. Heteroepitaxial ultrafine wire-like growth of InAs on GaAs substrates. *Appl. Phys. Lett.* **58,** 1080–1082 (1991).
3. Xia, Y. *et al.* One-dimensional nanostructures: Synthesis, characterization, and applications. *Adv. Mater.* **15,** 353–389 (2003).
4. Kuykendall, T., Ulrich, P., Aloni, S. & Yang, P. Complete composition tunability of InGaN nanowires using a combinatorial approach. *Nature Mater.* **6,** 951–956 (2007).
5. Wagner, R. S. & Ellis, W. C. Vapor-liquid-solid mechanism of single crystal growth. *Appl. Phys. Lett.* **4,** 89–90 (1964).
6. Morales, A. M. & Lieber, C. M. A laser ablation method for the synthesis of crystalline semiconductor nanowires. *Science* **279,** 208–211 (1998).
7. Yang, P. & Lieber, C. M. Nanorod-superconductor composites: a pathway to materials with high critical current densities. *Science* **273,** 1836–1840 (1996).
8. Wu, Y. & Yang, P. Direct observation of vapor–liquid–solid nanowire growth. *J. Am. Chem. Soc.* **123,** 3165–3166 (2001).
9. Björk, M. T. *et al.* One-dimensional heterostructures in semiconductor nanowhiskers. *Appl. Phys. Lett.* **80,** 1058–1060 (2002).
10. Wu, Y. & Yang, P. Germanium nanowire growth via simple vapor transport. *Chem. Mater.* **12,** 605–607 (2000).
11. Mølhave, K. *et al.* Epitaxial integration of nanowires in microsystems by local micrometer-scale vapor-phase epitaxy. *Small* **4,** 1741–1746 (2008).
12. Barrelet, C. J., Wu, Y., Bell, D. C. & Lieber, C. M. Synthesis of CdS and ZnS nanowires using single-source molecular precursors. *J. Am. Chem. Soc.* **125,** 11498–11499 (2003).
13. Radovanovic, P. V., Barrelet, C. J., Gradečak, S., Qian, F. & Lieber, C. M. General synthesis of manganese-doped II–VI and III–V semiconductor nanowires. *Nano Lett.* **5,** 1407–1411 (2005).
14. Johansson, J. *et al.* Structural properties of ⟨111⟩B-oriented III–V nanowires. *Nature Mater.* **5,** 574–580 (2006).
15. Mårtensson, T. *et al.* Epitaxial growth of indium arsenide nanowires on silicon using nucleation templates formed by self-assembled organic coatings. *Adv. Mater.* **19,** 1801–1806 (2007).
16. Duan, X. & Lieber, C. M. General synthesis of compound semiconductor nanowires. *Adv. Mater.* **12,** 298–302 (2000).
17. Pan, A., Liu, R., Sun, M. & Ning, C-Z. Quaternary alloy semiconductor nanobelts with bandgap spanning the entire visible spectrum. *J. Am. Chem. Soc.* **131,** 9502–9503 (2009).
18. Trentler, T. J. *et al.* Solution-liquid-solid growth of crystalline III–V semiconductors: an analogy to vapor-liquid-solid growth. *Science* **270,** 1791–1794 (1995).
19. Kuykendall, T. *et al.* Crystallographic alignment of high-density gallium nitride nanowire arrays. *Nature Mater.* **3,** 524–528 (2004).
20. Hochbaum, A. I., Fan, R., He, R. & Yang, P. Controlled growth of Si nanowire arrays for device integration. *Nano Lett.* **5,** 457–460 (2005).
21. He, R. *et al.* Si nanowire bridges in microtrenches: Integration of growth into device fabrication. *Adv. Mater.* **17,** 2098–2102 (2005).
22. Huang, M. H. *et al.* Room-temperature ultraviolet nanowire nanolasers. *Science* **292,** 1897–1899 (2001).
23. Yazawa, M., Koguchi, M., Muto, A., Ozawa, M. & Hiruma, K. Effect of one monolayer of surface gold atoms on the epitaxial growth of InAs nanowhiskers. *Appl. Phys. Lett.* **61,** 2051–2053 (1992).
24. Haraguchi, K., Katsuyama, T. & Hiruma, K. Polarization dependence of light emitted from GaAs p-n junctions in quantum wire crystals. *J. Appl. Phys.* **75,** 4220–4225 (1994).
25. Borgström, M. T., Immink, G., Ketelaars, B., Algra, R. & Bakkers, E. P. A. M. Synergetic nanowire growth. *Nature Nanotech.* **2,** 541–544 (2007).
26. Dick, K. A. *et al.* Failure of the vapor–liquid–solid mechanism in Au-assisted MOVPE growth of InAs nanowires. *Nano Lett.* **5,** 761–764 (2005).
27. Mårtensson, T. *et al.* Nanowire arrays defined by nanoimprint lithography. *Nano Lett.* **4,** 699–702 (2004).
28. Ertekin, E., Greaney, P. A., Chrzan, D. C. & Sands, T. D. Equilibrium limits of coherency in strained nanowire heterostructures. *J. Appl. Phys.* **97,** 114325 (2005).
29. Mårtensson, T. *et al.* Epitaxial III–V nanowires on silicon. *Nano Lett.* **4,** 1987–1990 (2004).
30. Tomioka, K., Motohisa, J., Hara, S. & Fukui, T. Control of InAs nanowire growth directions on Si. *Nano Lett.* **8,** 3475–3480 (2008).
31. Bakkers, E. P. A. M. *et al.* Epitaxial growth of InP nanowires on germanium. *Nature Mater.* **3,** 769–773 (2004).
32. Svensson, C. P. T. *et al.* Monolithic GaAs/InGaP nanowire light emitting diodes on silicon. *Nanotechnology* **19,** 305201 (2008).
33. Mandl, B. *et al.* Au-free epitaxial growth of InAs nanowires. *Nano Lett.* **6,** 1817–1821 (2006).
34. Ikejiri, K., Noborisaka, J., Hara, S., Motohisa, J. & Fukui, T. Mechanism of catalyst-free growth of GaAs nanowires by selective area MOVPE. *J. Cryst. Growth* **298,** 616–619 (2007).
35. Mohan, P., Motohisa, J. & Fukui, T. Controlled growth of highly uniform, axial/radial direction-defined, individually addressable InP nanowire arrays. *Nanotechnology* **16,** 2903–2907 (2005).
36. Mohan, P., Motohisa, J. & Fukui, T. Fabrication of InP/InAs/InP core–multishell heterostructure nanowires by selective area metalorganic vapor phase epitaxy. *Appl. Phys. Lett.* **88,** 133105 (2006).
37. Choi, H-J. *et al.* Self-organized GaN quantum wire UV lasers. *J. Phys. Chem. B* **107,** 8721–8725 (2003).
38. Qian, F. *et al.* Gallium nitride-based nanowire radial heterostructures for nanophotonics. *Nano Lett.* **4,** 1975–1979 (2004).
39. Qian, F. *et al.* Multi-quantum-well nanowire heterostructures for wavelength-controlled lasers. *Nature Mater.* **7,** 701–706 (2008).
40. Lauhon, L. J., Gudiksen, M. S., Wang, D. & Lieber, C. M. Epitaxial core–shell and core–multishell nanowire heterostructures. *Nature* **420,** 57–61 (2002).
41. Algra, R. E. *et al.* Twinning superlattices in indium phosphide nanowires. *Nature* **456,** 369–372 (2008).

42. Wu, Y., Fan, R. & Yang, P. Block-by-block growth of single-crystalline Si/SiGe superlattice nanowires. *Nano Lett.* **2,** 83–86 (2002).
43. Gudiksen, M. S., Lauhon, L. J., Wang, J., Smith, D. C. & Lieber, C. M. Growth of nanowire superlattice structures for nanoscale photonics and electronics. *Nature* **415,** 617–620 (2002).
44. Björk, M. T. *et al.* One-dimensional steeplechase for electrons realized. *Nano Lett.* **2,** 87–89 (2002).
45. Li, Y., Qian, F., Xiang, J. & Lieber, C. M. Nanowire electronic and optoelectronic devices. *Mater. Today* **9,** 18–27 (2006).
46. Dick, K. A. *et al.* Synthesis of branched 'nanotrees' by controlled seeding of multiple branching events. *Nature Mater.* **3,** 380–384 (2004).
47. Bierman, M. J., Lau, Y. K. A., Kvit, A. V., Schmitt, A. L. & Jin, S. Dislocation-driven nanowire growth and Eshelby twist. *Science* **320,** 1060–1063 (2008).
48. Zhu, J. *et al.* Formation of chiral branched nanowires by the Eshelby Twist. *Nature Nanotech.* **3,** 477–481 (2008).
49. Smith, P. A. *et al.* Electric-field assisted assembly and alignment of metallic nanowires. *Appl. Phys. Lett.* **77,** 1399–1401 (2000).
50. Huang, Y., Duan, X., Wei, Q. & Lieber, C. M. Directed assembly of one-dimensional nanostructures into functional networks. *Science* **291,** 630–633 (2001).
51. Messer, B., Song, J. H. & Yang, P. Microchannel networks for nanowire patterning. *J. Am. Chem. Soc.* **122,** 10232–10233 (2000).
52. Yang, P. Nanotechnology: Wires on water. *Nature* **425,** 243–244 (2003).
53. Tao, A. R., Huang, J. & Yang, P. Langmuir–Blodgettry of nanocrystals and nanowires. *Acc. Chem. Res.* **41,** 1662–1673 (2008).
54. Ahn, J-H. *et al.* Heterogeneous three-dimensional electronics by use of printed semiconductor nanomaterials. *Science* **314,** 1754–1757 (2006).
55. Ashkin, A., Dziedzic, J. M., Bjorkholm, J. E. & Chu, S. Observation of a single-beam gradient force optical trap for dielectric particles. *Opt. Lett.* **11,** 288–290 (1986).
56. Grier, D. G. A revolution in optical manipulation. *Nature* **424,** 810–816 (2003).
57. Korda, P., Spalding, G. C., Dufresne, E. R. & Grier, D. G. Nanofabrication with holographic optical tweezers. *Rev. Sci. Instrum.* **73,** 1956–1957 (2002).
58. Pauzauskie, P. J. *et al.* Optical trapping and integration of semiconductor nanowire assemblies in water. *Nature Mater.* **5,** 97–101 (2006).
59. Agarwal, R. *et al.* Manipulation and assembly of nanowires with holographic optical traps. *Opt. Express* **13,** 8906–8912 (2005).
60. Chiou, P. Y., Ohta, A. T. & Wu, M. C. Massively parallel manipulation of single cells and microparticles using optical images. *Nature* **436,** 370–372 (2005).
61. Jamshidi, A. *et al.* Dynamic manipulation and separation of individual semiconducting and metallic nanowires. *Nature Photon.* **2,** 86–89 (2008).
62. Yan, H. *et al.* Dendritic nanowire ultraviolet laser array. *J. Am. Chem. Soc.* **125,** 4728–4729 (2003).
63. Sirbuly, D. J., Law, M., Yan, H. & Yang, P. Semiconductor nanowires for subwavelength photonics integration. *J. Phys. Chem. B* **109,** 15190–15213 (2005).
64. Johnson, J. C., Yan, H., Yang, P. & Saykally, R. J. Optical cavity effects in ZnO nanowire lasers and waveguides. *J. Phys. Chem. B* **107,** 8816–8828 (2003).
65. Zapien, J. A. *et al.* Room-temperature single nanoribbon lasers. *Appl. Phys. Lett.* **84,** 1189–1191 (2004).
66. Duan, X., Huang, Y., Agarwal, R. & Lieber, C. M. Single-nanowire electrically driven lasers. *Nature* **421,** 241–245 (2003).
67. Johnson, J. C. *et al.* Single gallium nitride nanowire lasers. *Nature Mater.* **1,** 106–110 (2002).
68. Chin, A. H. *et al.* Near-infrared semiconductor subwavelength-wire lasers. *Appl. Phys. Lett.* **88,** 163115 (2006).
69. Pauzauskie, P. J., Sirbuly, D. J. & Yang, P. Semiconductor nanowire ring resonator laser. *Phys. Rev. Lett.* **96,** 143903 (2006).
70. Zimmler, M. A., Bao, J., Capasso, F., Müller, S. & Ronning, C. Laser action in nanowires: Observation of the transition from amplified spontaneous emission to laser oscillation. *Appl. Phys. Lett.* **93,** 051101 (2008).
71. Barrelet, C. J. *et al.* Hybrid single-nanowire photonic crystal and microresonator structures. *Nano Lett.* **6,** 11–15 (2006).
72. Maslov, A. V. & Ning, C. Z. Far-field emission of a semiconductor nanowire laser. *Opt. Lett.* **29,** 572–574 (2004).
73. van Vugt, L. K., Rühle, S. & Vanmaekelbergh, D. Phase-correlated nondirectional laser emission from the end facets of a ZnO nanowire. *Nano Lett.* **6,** 2707–2711 (2006).
74. Hua, B., Motohisa, J., Kobayashi, Y., Hara, S. & Fukui, T. Single GaAs/GaAsP coaxial core–shell nanowire lasers. *Nano Lett.* **9,** 112–116 (2009).
75. Sköld, N. *et al.* Growth and optical properties of strained GaAs-$Ga_xIn_{1-x}P$ core–shell nanowires. *Nano Lett.* **5,** 1943–1947 (2005).
76. Hua, B., Motohisa, J., Ding, Y., Hara, S. & Fukui, T. Characterization of Fabry-Pérot microcavity modes in GaAs nanowires fabricated by selective-area metal organic vapor phase epitaxy. *Appl. Phys. Lett.* **91,** 131112 (2007).
77. Duan, X., Huang, Y., Cui, Y., Wang, J. & Lieber, C. M. Indium phosphide nanowires as building blocks for nanoscale electronic and optoelectronic devices. *Nature* **409,** 66–69 (2001).
78. Huang, Y., Duan, X. & Lieber, C. M. Nanowires for integrated multicolor nanophotonics. *Small* **1,** 142–147 (2005).
79. Zhong, Z., Qian, F., Wang, D. & Lieber, C. M. Synthesis of p-type gallium nitride nanowires for electronic and photonic nanodevices. *Nano Lett.* **3,** 343–346 (2003).
80. Minot, E. D. *et al.* Single quantum dot nanowire LEDs. *Nano Lett.* **7,** 367–371 (2007).
81. Law, M. *et al.* Nanoribbon waveguides for subwavelength photonics integration. *Science* **305,** 1269–1273 (2004).
82. O'Brien, J. L., Pryfde, G. J., White, A. G., Ralph, T. C. & Branning, D. Demonstration of an all-optical quantum controlled-NOT gate. *Nature* **426,** 264–267 (2003).
83. Ibrahim, T. A. *et al.* All-optical switching in a laterally coupled microring resonator by carrier injection. *IEEE Photon. Technol. Lett.* **15,** 36–38 (2003).
84. Tong, L. *et al.* Subwavelength-diameter silica wires for low-loss optical wave guiding. *Nature* **426,** 816–819 (2003).
85. Sirbuly, D. J. *et al.* Optical routing and sensing with nanowire assemblies. *Proc. Natl Acad. Sci. USA* **102,** 7800–7805 (2005).
86. Nakayama, Y. *et al.* Tunable nanowire nonlinear optical probe. *Nature* **447,** 1098–1101 (2007).
87. Kind, H., Yan, H., Messer, B., Law, M. & Yang, P. Nanowire ultraviolet photodetectors and optical switches. *Adv. Mater.* **14,** 158–160 (2002).
88. Wang, J., Gudiksen, M. S., Duan, X., Cui, Y. & Lieber, C. M. Highly polarized photoluminescence and photodetection from single indium phosphide nanowires. *Science* **293,** 1455–1457 (2001).
89. Gu, Y. *et al.* Near-field scanning photocurrent microscopy of a nanowire photodetector. *Appl. Phys. Lett.* **87,** 043111 (2005).
90. Hayden, O., Agarwal, R. & Lieber, C. M. Nanoscale avalanche photodiodes for highly sensitive and spatially resolved photon detection. *Nature Mater.* **5,** 352–356 (2006).
91. Campbell, J. C. Recent advances in telecommunications avalanche photodiodes. *J. Lightwave Technol.* **25,** 109–121 (2007).
92. Hayden, O. & Payne, C. K. Nanophotonic light sources for fluorescence spectroscopy and cellular imaging. *Angew. Chem. Int. Ed.* **44,** 1395–1398 (2005).
93. O'Regan, B. & Grätzel, M. A low-cost, high-efficiency solar cell based on dye-sensitized colloidal TiO_2 films. *Nature* **353,** 737–740 (1991).
94. Law, M., Greene, L. E., Johnson, J. C., Saykally, R. & Yang, P. Nanowire dye-sensitized solar cells. *Nature Mater.* **4,** 455–459 (2005).
95. Law, M. *et al.* ZnO-Al_2O_3 and ZnO-TiO_2 core–shell nanowire dye-sensitized solar cells. *J. Phys. Chem. B* **110,** 22652–22663 (2006).
96. Tian, B. *et al.* Coaxial silicon nanowires as solar cells and nanoelectronic power sources. *Nature* **449,** 885–889 (2007).
97. Murashov, V. & Howard, J. The US must help set international standards for nanotechnology. *Nature Nanotech.* **3,** 635–636 (2008).
98. Maslov, A. V. & Ning, C. Z. Size reduction of a semiconductor nanowire laser by using metal coating. *Proc. SPIE* **6468,** 64680I (2007).
99. Hill, M. T. *et al.* Lasing in metallic-coated nanocavities. *Nature Photon.* **1,** 589–594 (2007).
100. Oulton, R. F., Sorger, V. J., Genov, D. A., Pile, D. F. P. & Zhang, X. A hybrid plasmonic waveguide for subwavelength confinement and long-range propagation. *Nature Photon.* **2,** 496–500 (2008).

Acknowledgements

The authors would like to acknowledge here contributions of members of our research group and collaborators on this nanowire photonics programme. This work was supported by the Office of Basic Science, US Department of Energy and the Defense Advanced Research Projects Agency. P.Y. would like to thank the National Science Foundation for the A.T. Waterman Award.